Available online at www.sciencedirect.com
SCIENCE DIRECT
Robotics and Autonomous Systems 54 (2006) 461–471
Robotics and Autonomous Systems
www.elsevier.com/locate/robot

Optical guidance method for robots capable of vision and communication

Igor E. Paromtchik*

RIKEN, 2-1 Hirosawa, Wako-shi, Saitama 351-0198, Japan

Received 11 December 2004; received in revised form 27 July 2005; accepted 1 February 2006
Available online 3 April 2006

Abstract

The optical guidance of robots spans the research topics of robotics, computer vision, communication and real-time control. The proposed method aims to improve the accuracy of guidance along a desired route in an environment that is unknown to the robot. The key idea is to indicate the numerical coordinates of target positions by means of projecting a laser light onto the ground. In contrast with other guidance methods, which communicate the target position numerically, using optical commands avoids the need to maintain the coordinate transformation between the robot's system and that of the environmental model ("world" reference coordinates). The image processing and communication ensure that the robot accurately follows the route indicated by laser beacons, and self-localization becomes less relevant for guidance. The experimental results have proved the effectiveness of this method.

Keywords: Mobile robot; Optical guidance; Laser

1. Introduction

Guidance means *show the way while in motion*, and localization is to *confine within a particular area* [1]. Guidance is passive if no localization of the guided objects is performed, e.g. a lighthouse guiding ships, and is active when it relies on communication with the guided objects and their localization. This paper introduces an optical guidance method that represents an active guidance concept. The method provides guidance of mobile and humanoid robots in an environment that is unknown to the robots.

The motivation for this work originates in our experiments on teleoperation of wheeled robots, where the robot pose (position and orientation) is obtained from dead-reckoning and is transmitted to the teleoperation system for updating the pose in the environmental model. The human operator uses this model to control the robot remotely. However, accumulation of positional and orientational errors caused by the wheels sliding on the ground and inaccurate modeling results in a discrepancy between the actual robot pose in the environment and its estimate in the model. Accumulation of this discrepancy over time makes teleoperation impossible from some instant, because of the danger of collision with the environment.

The proposed method aims to eliminate this discrepancy from the guidance. The novelty of this work is supported by our patents [2,3]. The key idea of the method is to show the target position instead of commanding it numerically. This is achieved by means of projecting a laser light onto the ground, as sketched in Fig. 1 in Section 3. The guidance system operates with the environmental model and comprises a computer-controlled laser pointer that directs a laser beam onto desired positions. The guidance system communicates with the robot when indicating the target position and receiving an update from the robot on attaining this position. The robot's vision system processes the color images in order to detect the laser beacon and evaluate its relative coordinates. The robot's controller drives the vehicle toward the beacon. The guidance system controls the orientation and lighting of the laser in order to indicate target positions—one at each instant along the planned route. When the robot reaches the proximity of the beacon, the guidance system shows the next target position, and the robot continuously follows the path [4].

The main advantage of this method is the improved *accuracy of guidance*. It also allows *implicit localization* of the robot within the environment: when the robot has reached its indicated target position and has confirmed this to the

* Tel.: +81 48 462 1111x7413; fax: +81 48 467 7248.
E-mail address: igor.paromtchik@ieee.org.

0921-8890/$ - see front matter © 2006 Published by Elsevier B.V.
doi:10.1016/j.robot.2006.02.005

guidance system, an adequate estimate of its coordinates in the environmental model is known. Since the control system of the robot operates with the relative coordinates of target positions obtained from image processing, the transformation between the coordinate system of the environmental model ("world" reference coordinates) and that of the robot, as well as self-localization by the robot, become less relevant for guidance.

The communication ability and updating of the environmental model by the guidance system allows us to use it as a *mediator* for cooperative multiple robots [5]. For instance, the sensor data gathered by the robots and stored in the environmental model is available to all robots in the fleet, i.e. cooperative knowledge acquisition and sharing can be achieved. The distribution of tasks and their allocation to the robots is performed with the use of the environmental model as a part of the guidance system. One robot can request the system to guide another robot to a specified destination. The multi-robot system becomes more efficient and robust and enhances the capabilities of any individual robot by assisting the robot in reaching its destination in an unknown environment and facilitating the sharing of environmental data among robots.

This paper focuses on the optical guidance method. Its feasibility is shown in an example of laser guidance of an omnidirectional mobile robot. The paper is organized as follows. The related works on guidance of robots are discussed in Section 2. The concept of optical guidance and the kinematic models are presented in Section 3. The operation of the guidance system and the communication diagrams are considered in Section 4. The path computation by the guidance system and motion generation by the robot are explained in Section 5. The implementation and experimental results are described in Section 6. The conclusions are given in Section 7.

2. Related works

Robot guidance involves various tasks such as: teleoperation, communication, environment modeling, motion planning, image processing, fusion of sensor data, and real-time control for path tracking and navigation. This section deals with the methods that are closely related to optical guidance, while reviews of other navigation methods and sensors can be found in [6] and [7].

Simultaneous localization and mapping (SLAM) improves the performance of a mobile robot while navigating in an uncertain or unknown environment [8–11]. The robot explores the environment, builds the map and, concurrently, navigates without external guidance. The target position is commanded explicitly (in most cases, numerically) in a reference coordinate system. SLAM serves to maintain accurate transformation between the robot's coordinate system and the reference system. This is required in order to enable the robot to attain the given target position. In contrast, the proposed guidance method communicates the target position optically (not numerically), allowing us to avoid transformations between the coordinate systems and the need for self-localization of the robot.

Visual servoing makes use of image processing to control the robot relative to a landmark [12,13]. The target position is specified by the target image, which must be captured from this position in advance. The objective during visual servoing is to achieve convergence of the current image taken by the robot toward the target image by means of controlling the robot motion. As a result, the robot attains its target position. The optical guidance differs from visual servoing because it produces laser beacons which indicate a feasible route in the environment. Besides, communication between the guidance system and the robot ensures that the next target position is commanded when the robot has reached its current target position or its proximity.

The use of a laser light to indicate an area of interest has various applications. For instance, environment recognition with the use of a laser pointer is discussed in [14]. The human operator or a "manager" mobile robot directs the laser pointer onto an object, and two "worker" mobile robots, each equipped with a color CCD camera, detect the flashing laser light. Obtaining the relative coordinates of the laser spot by means of stereo vision requires that the precise poses of the "worker" robots are known. However, precise localization of mobile robots is no trivial task [6] and the "self-positioning" of robots with on-board markers [14] relies on human assistance.

Guidance by means of information support from sensor devices distributed in an "intelligent space" is studied in [15]. The visual sensors watch robots and guide them in a networked environment. Each robot is identified by a color bar code stored in the database. The robot is localized by one of the visual sensors by means of measuring the distance between the robot and the sensor. Since the pose estimation error increases with the distance, each visual sensor serves its proximity area. Given the desired path and the estimated pose, the control command is computed and transmitted to the robot via a wireless local area network (LAN). Guidance based on localization and communication is achieved, however position estimation errors can be as large as 17 cm [15].

A system with a laser attached to one of two Canon VC-C1 communication cameras placed on a robot manipulator is described in [16]. The laser is precisely aligned with the optical axis of its camera and is centered over the top of the camera lens. The purpose of this system is to provide convergence of the cameras on the object being viewed. The use of a laser light provides to measure the distance more accurately to the object being viewed. The reported accuracy of the distance calculation between the camera and the laser spot on the surface is to roughly the nearest tenth of an inch.

A computer-servoed laser pointer projects the spot of light at the user-specified locations on the surface of interest for camera-space manipulation in [17]. The light spots serve as the common camera-space points which are necessary to establish mapping between the cameras viewing the workspace of the manipulator. The high precision of positioning and orienting the manipulator's end effector is achieved by using a method of camera-space manipulation.

Numerous publications address tracking a reference path by a mobile robot. The path is specified by a guidance

line or, for example, magnetic markers in the ground. The on-board displacement sensor measures the tracking error, and the controller issues the adequate steering commands [18]. In contrast, the proposed method focuses on guidance (i.e. providing a feasible reference path) where tracking the laser beacons relies on image processing by the robot and communication between the guidance system and the robot. This ensures that the next target position is shown when the robot has reached the proximity of its current target position and has confirmed this to the guidance system. As a result, the guidance accuracy is improved. Besides, the optical guidance allows us to modify the reference path flexibly.

The advantage of the proposed optical guidance method is due to the following features: target positions are indicated precisely in the environment by means of computer-servoing the laser pointer or pointers situated in the environment; visual feedback provides better positioning accuracy of the robot; the path to follow is indicated interactively as a sequence of target positions (laser beacons); accumulation of errors caused by dead-reckoning does not influence localization of the robot in the environment, because the localization is performed when the robot has attained its indicated target position; communication between the guidance system and the robot allows knowledge acquisition and sharing in the case of cooperative multiple robots; and one guidance system can indicate target positions for multiple robots. These features are addressed in the subsequent sections, except for cooperative multiple robots.

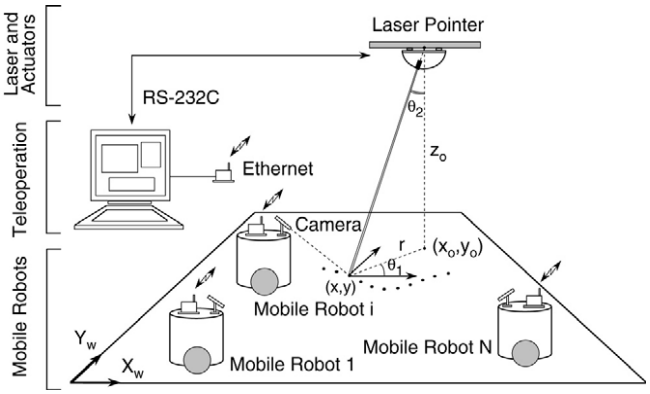

Fig. 1. A sketch of a laser guidance system.

Fig. 2. A laser pointer mounted onto the pan-tilt mechanism of a Canon VC-C1 communication camera.

3. Models

The guidance system indicates target positions for the robot by means of a laser light projected onto the ground [4]. The approach is sketched in Fig. 1, where the overall system involves: the laser, the teleoperation board, and the mobile robots. The guidance system comprises the teleoperation board and the laser pointer with its actuators—at least two degrees of freedom are required in order to direct the optical axis of the laser to any position on the ground. The coordinates of the target positions are computed from the environmental model according to the motion task, or they are set by an operator. The guidance system relies on wireless communication with the control systems of the robots. The robot's vision system processes color images to detect the laser beacon on the ground and evaluate its relative coordinates. The relevant part of the environmental model along a route is updated with robot sensor data. In order to avoid occlusion of laser beacons in cluttered areas, two or more laser pointers are used, e.g. pointers are placed at opposite corners of the work area. The laser pointer can also be mounted onto mobile robots in a multi-robot scenario or attached to the manipulator with redundant degrees of freedom [2].

3.1. Guidance system model

Let the laser pointer be mounted onto a pan-tilt mechanism, and $\mathbf{\Theta} = (\theta_1, \theta_2)^T$ denote the rotation angles of this mechanism, where θ_1 and θ_2 are the pan and tilt angles, respectively. Let the initial angles be $\theta_1 = \theta_2 = 0$. Let the "rotation point" of the pan-tilt mechanism be situated at a height z_o and its ground coordinates be denoted (x_o, y_o), as shown in Fig. 1. Let $\mathbf{X} = (x, y)^T$ denote the position of the laser beacon on the ground.

Obtain a kinematic model of a guidance system where the laser pointer is mounted onto the pan-tilt mechanism of a Canon VC-C1 communication camera, shown in Fig. 2. Let the pan angle be counted relative to the vertical plane which involves the rotation point of the pan-tilt mechanism and the origin of the ground coordinate system. Let a constant offset of the pan angle be $\alpha_o = \arctan \frac{y_o}{x_o}$. Let β_o denote an angle between the support base of the pan-tilt mechanism and a vertical line (the same angle β_o is between the laser optical axis in the initial position $\theta_1 = \theta_2 = 0$ and a vertical line). Let b_o denote a distance between the rotation point and the laser optical axis.

A position of the laser beacon on the ground is

$$\mathbf{X} = \begin{pmatrix} x_o - (z_o \tan\theta_2' + b_o/\cos\theta_2')\cos\theta_1' \\ y_o - (z_o \tan\theta_2' + b_o/\cos\theta_2')\sin\theta_1' \end{pmatrix}, \tag{1}$$

where:

$$\theta_1' = \theta_1 + \alpha_o, \tag{2}$$

$$\theta_2' = \theta_2 + \beta_o, \quad -\beta_o < \theta_2 < \frac{\pi}{2},\ 0 < \beta_o < \frac{\pi}{2}. \tag{3}$$

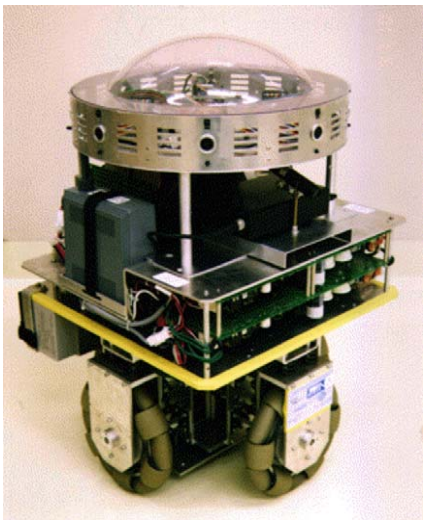

Fig. 3. The omni-directional mobile robot.

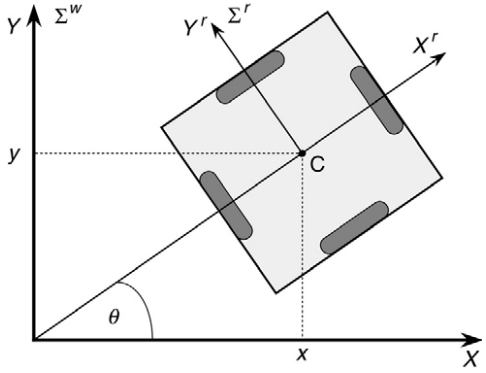

Fig. 4. A kinematic model of the omni-directional mobile robot.

The pan angle is

$$\theta_1(x, y) = \arctan \frac{y_o - y}{x_o - x} - \alpha_o. \tag{4}$$

Using (3) and an equation $z_o \tan\theta_2' + \frac{b_o}{\cos\theta_2'} = r$, one can derive the tilt angle:

$$\theta_2(x, y) = \arctan \frac{r}{z_o} - \arcsin \frac{b_o}{\sqrt{r^2 + z_o^2}} - \beta_o. \tag{5}$$

The Eqs. (4) and (5) allow us to compute $\boldsymbol{\Theta} = \boldsymbol{\Theta}(\mathbf{X})$ in order to direct the laser beam onto the position $\mathbf{X}$ on the ground. Note that, if $\alpha_o = \beta_o = b_o = 0$, Eqs. (4) and (5) describe the configuration shown in Fig. 1.

3.2. Mobile robot model

Our mobile robot is shown in Fig. 3. The robot is equipped with four omni-directional wheels and can move in two directions and rotate simultaneously. The kinematic model of the vehicle is depicted in Fig. 4. The coordinates of the robot relative to a reference coordinate system $\boldsymbol{\Sigma}^w$ are denoted as (x, y, θ), where $x = x(t)$ and $y = y(t)$ are the coordinates of the intersection point C of the imaginary axes connecting the wheel centers of each pair of the parallel wheels, $\theta = \theta(t)$ is the orientation of the robot, and t is time. The translation along each direction and rotation with respect to $\boldsymbol{\Sigma}^r$ are decoupled and can be driven by the corresponding actuators [19].

The kinematic model of the robot is described by the following equations:

$$\begin{cases} \dot{x} = v_x \cos\theta - v_y \sin\theta, \\ \dot{y} = v_x \sin\theta + v_y \cos\theta, \\ \dot{\theta} = \omega, \end{cases} \tag{6}$$

where v_x and v_y denote the robot velocities in the longitudinal and lateral directions, respectively, in the robot's coordinate system, ω is the rotational velocity, and θ is the orientation angle. Note that, if the constraint $v_y = 0$ is set in (6), this results in a non-holonomic model.

Eq. (6) allows us to evaluate the translational and rotational velocities of the robot and estimate its pose with respect to $\boldsymbol{\Sigma}^w$. The model (6) enables us to obtain the robot's coordinates in the "world" coordinate system. This model is valid for a vehicle moving on flat ground with a pure rolling contact without slippage between the wheels and the ground. However, these requirements cannot be fulfilled in practice, which results in the discrepancy between the actual robot pose in the environment and its estimation in the model. The proposed optical guidance method aims to eliminate this discrepancy from the guidance process.

4. Event-based guidance

Let a desired path $\mathbf{X}(t) = [x(t), y(t)]^T$ be indicated by means of the laser beacons which are separated by a distance step $\Delta X_s > 0$, as shown in Fig. 5, where the actual path of the robot is denoted $\mathbf{X}_r(t) = [x_r(t), y_r(t)]^T$. When the robot reaches the ΔX_s-proximity of its target position, a new target position is set. Tracking the desired path $\mathbf{X}(t)$ is achieved if

$$\lim_{t\to\infty} |\mathbf{X}(t) - \mathbf{X}_r(t)| \le \varepsilon, \tag{7}$$

where $\varepsilon > 0$ is a given constant.

The position of the laser beacon is obtained from image processing. The relative coordinates of the beacon are distances

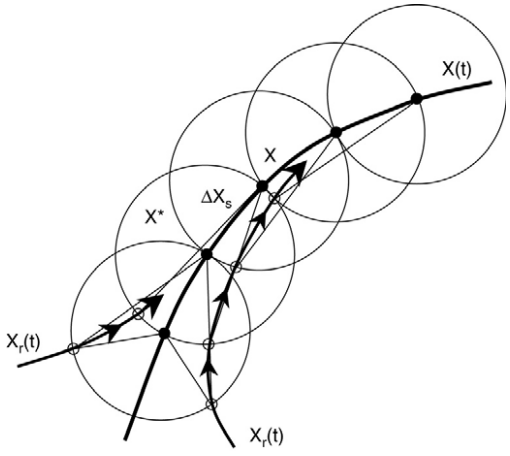

Fig. 5. The desired path $\mathbf{X}(t)$ is indicated by laser beacons at a distance step ΔX_s, and $\mathbf{X}_r(t)$ is the actual path of the robot approaching the desired path either from the left or right side.

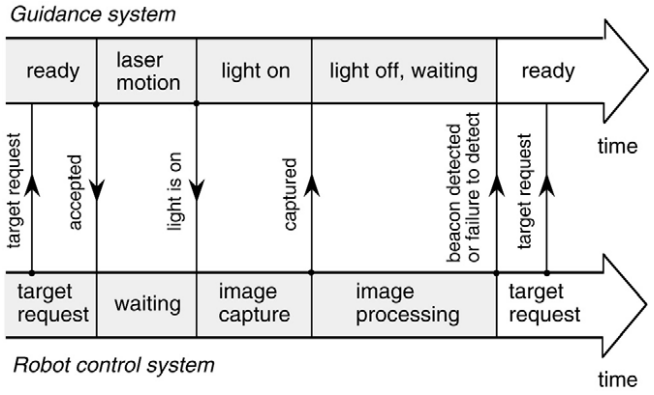

Fig. 6. Communication diagram I.

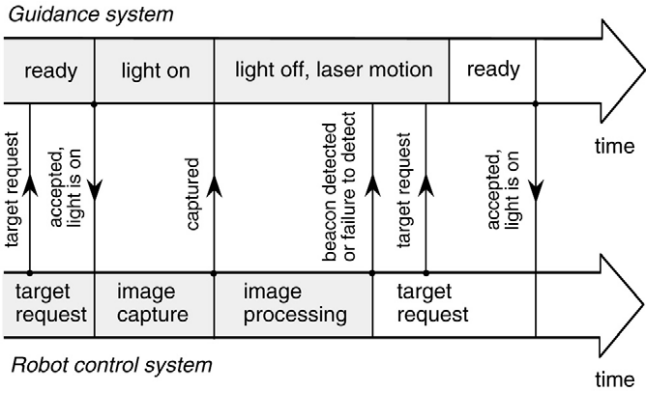

Fig. 7. Communication diagram II.

d_x and d_y in the longitudinal and lateral directions respectively, as seen by the robot camera. The orientation error is computed as $\theta_e = \arctan \frac{d_y}{d_x}$ and is compensated in order to direct the vehicle toward the beacon. The control system of the robot generates trajectories in the (x, y, θ)-coordinates and drives the vehicle to the beacon. The distance between the robot and its target position during path tracking is bounded by $2\Delta X_s$, as seen in Fig. 5.

4.1. Communication for guidance

The diagram in Fig. 6 illustrates communication between the robot control system and the guidance system. Initially, the robot sends a target request to the guidance system. The request is accepted and the system orients the laser pointer appropriately in order to show a target position. The laser light is turned on, and the robot is informed that the target position is being indicated. The image is captured by the robot's vision system, and the image processing starts. The laser light is turned off. Image processing results in either detection of the beacon or failure. Whatever happens, the robot control system sends the corresponding information to the guidance system along with a target request. In the case of failure to detect the beacon, the guidance system performs a failure compensation procedure (e.g. the target is set closer to the robot, or the additional laser pointer is used to avoid occlusion). The shaded areas in Fig. 6 show the time period of this *event-based guidance*, from requesting a target position to obtaining results of image processing.

Let $\tau_s > 0$ denote a motion time for a transition of the laser beacon from a position $\mathbf{X}^\star$ to a target position $\mathbf{X}$, shown in Fig. 5. The period τ_s is a variable delay that also includes time for oscillations in the pan-tilt mechanism to abate. When the image is captured, let the subsequent processing time period equate to $\tau_p > 0$, which is also variable. The periods τ_s and τ_p must be shortened, because they represent the waiting periods of the robot and the guidance system, respectively. For instance, the laser pointer can be re-oriented without waiting for the results of image processing—the corresponding diagram is shown in Fig. 7. When image processing terminates, the laser pointer is ready to show the next target position to the robot. Note that this operation requires the reliable detection of laser beacons.

The indication and detection of the target positions must be fast enough to ensure continuous motion of the robot along the path, i.e. $\tau_s + \tau_p < \tau_r$ (diagram I) or $\max(\tau_s, \tau_p) < \tau_r$ (diagram II), where $\tau_r > 0$ is a period corresponding to robot motion over a distance ΔX_s. Also, the laser beacon should appear at such a look-ahead distance in front of the vehicle where it can be detected reliably.

5. Path computation

The guidance system operates with the environmental model and computes the path for the robot to follow. This path is further indicated to the robot by means of laser beacons. The robot's control system detects the beacon, evaluates its relative coordinates, and issues the control commands for the servo-systems. Obtaining the path by the guidance system and motion generation by the robot's control system are discussed in this section.

5.1. Guidance path

A heuristic search is performed in the environmental model to find a coarse route to the destination. The search results in a set of subgoals $\mathbf{X}_k = (x_k, y_k)^T$, $k = 0, 1, \ldots, n$, representing the planned route. The guidance path $\mathbf{X}(t) = [x(t), y(t)]^T$, $t \in [T_1, T_2]$, is obtained by means of a spline-interpolation:

$$\mathbf{X}(t) = \sum_{i=0}^{3} \mathbf{A}_{ki} \left(\frac{t - t_k}{h_k} \right)^i, \quad t \in \left[t_k, t_{k+1} \right], \tag{8}$$

where $\mathbf{A}_{ki} = (a_{ki}^x, a_{ki}^y)^T$ is a matrix of coefficients, $h_k = t_{k+1} - t_k$, $k = 0, 1, \ldots, n-1$ and $T_1 = t_0 < t_1 < \cdots < t_n = T_2$. The initial and final conditions are: $\mathbf{X}(T_1) = \mathbf{X}_0$, $\dot{\mathbf{X}}(T_1) = 0$, $\mathbf{X}(T_2) = \mathbf{X}_n$, $\dot{\mathbf{X}}(T_2) = 0$, and an auxiliary point is introduced: $\mathbf{X}_{n+1} = \mathbf{X}_{n-1}$. The coefficients of (8) are:

$$\mathbf{A}_{k0} = \mathbf{X}_k, \tag{9}$$

$$\mathbf{A}_{k1} = h_k \dot{\mathbf{X}}_k, \tag{10}$$

$$\mathbf{A}_{k2} = \frac{h_k + 2h_{k+1}}{h_{k+1}} (\mathbf{X}_{k+1} - \mathbf{X}_k) - \frac{h_k^2}{h_{k+1}(h_k + h_{k+1})} (\mathbf{X}_{k+2} - \mathbf{X}_k) - 2h_k \dot{\mathbf{X}}_k, \tag{11}$$

$$\mathbf{A}_{k3} = -\frac{h_k + h_{k+1}}{h_{k+1}}(\mathbf{X}_{k+1} - \mathbf{X}_k) + \frac{h_k^2}{h_{k+1}(h_k + h_{k+1})}(\mathbf{X}_{k+2} - \mathbf{X}_k) + h_k\dot{\mathbf{X}}_k. \quad (12)$$

The coefficients (9)–(12) provide the continuity of $\mathbf{X}(t)$ and $\dot{\mathbf{X}}(t)$ for $t \in [T_1, T_2]$. The guidance system indicates target positions along a path $\mathbf{X}(t)$ at a distance step ΔX_s which is set according to a desired precision.

5.2. Motion generation

The motion generation aims to obtain the smooth functions $x_r(t)$, $y_r(t)$ and $\theta_r(t)$ in order to drive the vehicle from its current position $\mathbf{X}_r = (x_r, y_r)^T$ to a target position $\mathbf{X}_d$, where the laser beacon is detected. Cubic interpolation is used, and the smooth trajectories ensure minimal accelerations and slippage. Motion generation is performed in the coordinate system of the robot, while the guidance path is computed in the "world" reference coordinates of the environmental model.

Consider a polynomial

$$\mathbf{X}_r(t) = \sum_{i=0}^{3} \mathbf{A}_i \left(\frac{t}{T}\right)^i, \quad 0 \le t \le T, \quad (13)$$

with the boundary conditions: $\mathbf{X}_r(0) = \mathbf{X}_o$, $\mathbf{X}_r(T) = \mathbf{X}_T$, $\dot{\mathbf{X}}_r(0) = \dot{\mathbf{X}}_o$, $\dot{\mathbf{X}}_r(T) = \dot{\mathbf{X}}_T$, where $T > 0$ is the interpolation period, and $\mathbf{A}_i = (a_i^x, a_i^y)^T$ is a matrix of coefficients. Let $\mathbf{X}_T$ be an auxiliary point between positions $\mathbf{X}_r$ and $\mathbf{X}_d$ such that $\Delta\mathbf{X}_T = \mathbf{X}_T - \mathbf{X}_o$ satisfies the following condition:

$$|\Delta\mathbf{X}_T| \ll |\mathbf{X}_d - \mathbf{X}_r|. \quad (14)$$

Let the coefficients $\mathbf{A}_i$ be recomputed with a sampling period $T^\star$ such that $0 < T_s < T^\star \ll T$, while T_s, T, $\dot{\mathbf{X}}_T$, and $\Delta\mathbf{X}_T$ are constant. Note that the recomputation of $\mathbf{A}_i$ with the sampling period $T^\star$ interrupts the interpolation that was intended for a period T.

Let the appropriations $\mathbf{X}_o := \mathbf{X}_r(kT^\star)$, $\dot{\mathbf{X}}_o := \dot{\mathbf{X}}_r(kT^\star)$, $\mathbf{X}_T := \mathbf{X}_r(kT^\star) + \Delta\mathbf{X}_T$, $k = 1, 2, \ldots$ ensure the continuity of $\mathbf{X}_r(t)$ and $\dot{\mathbf{X}}_r(t)$ at the boundary between subsequent computations $(k-1)$ and k. Let the recomputation of $\mathbf{A}_i$ be performed until the robot reaches the proximity of $\mathbf{X}_d$:

$$|\mathbf{X}_d - \mathbf{X}_r(kT^\star)| \le \Delta X_s^\star, \quad (15)$$

where $|\Delta\mathbf{X}_T| < \Delta X_s^\star < \Delta X_s$. The orientation $\theta_r(t)$ is computed according to the equation similar to (13) with conditions that are similar to (14) and (15).

This motion generation is illustrated in Fig. 8 for the x-coordinate. Each k-th interpolation step is performed to a virtual point situated at a distance Δx_T from the actual position. The virtual point is shifted with a sampling period $T^\star$ in the direction of x_d, and the coefficients a_i^x are recomputed [3,20].

This motion generation has a property that, for a given $\dot{\mathbf{X}}_d$, the following velocity condition holds for $n > k$:

$$|\dot{\mathbf{X}}_d - \dot{\mathbf{X}}_r(nT^\star)| < \varepsilon, \quad (16)$$

where $\varepsilon > 0$ is a small constant, and

$$|\ddot{\mathbf{X}}_r(t)| \le \ddot{x}_{\max}, \quad (17)$$

where $\ddot{x}_{\max} > 0$ is a given constant.

Let us prove (16) and (17) for the one-dimensional case of the x-coordinate. When the coefficients $a_i = a_i^x$ are recomputed with the sampling period $T^\star$, one can derive $\dot{x}_r(kT^\star)$ from (13), omitting the index r:

$$\dot{x}(kT^\star) = b^k\dot{x}_0 + c\left(1 + \sum_{i=1}^{k-1} b^i\right), \quad (18)$$

where $b = 1 - 4\tau + 3\tau^2$, $c = 6(1-\tau)\tau v - 3(2-\tau)\tau\dot{x}_T$, and the following notations are used: $v = \frac{\Delta x_T}{T}$ and $\tau = \frac{T^\star}{T} \ll 1$. Because $0 < b < 1$, the limit value of $\dot{x}(kT^\star)$ in Eq. (18) is [21]:

$$\lim_{k\to\infty} \dot{x}(kT^\star) = \frac{c}{1-b}. \quad (19)$$

Taking into account that $\dot{x}_T$ is an auxiliary constant, one can choose $\dot{x}_T = 0$ and rewrite (19) as

$$\lim_{k\to\infty} \dot{x}(kT^\star) = \frac{6(1-\tau)}{4-3\tau}v. \quad (20)$$

If v is computed as $v = \frac{4-3\tau}{6(1-\tau)}\dot{x}_d$, Eq. (20) becomes:

$$\lim_{k\to\infty} \dot{x}(kT^\star) = \dot{x}_d. \quad (21)$$

Eq. (21) proves the convergence of $\dot{\mathbf{X}}_r(t)$ to $\dot{\mathbf{X}}_d$ as in (16) and allows us to set the first derivative while interpolating by means of a cubic polynomial. Note that this property is not apparent for the cubic interpolation, but is a result of our interpolation method [3]. This property is used to set the velocity of the robot, as described in Section 6.2.

The second derivative is obtained as

$$\ddot{x}(kT^\star) = \frac{(4-3\tau)\dot{x}_d}{6(1-\tau)\Delta x_T} \cdot \left(\frac{4-3\tau}{1-\tau}\dot{x}_d - 4\dot{x}(kT^\star)\right). \quad (22)$$

The value of $\ddot{x}(t)$ depends on a deviation between $\dot{x}_d$ and $\dot{x}(t)$. Taking into account (16), one can conclude that this deviation

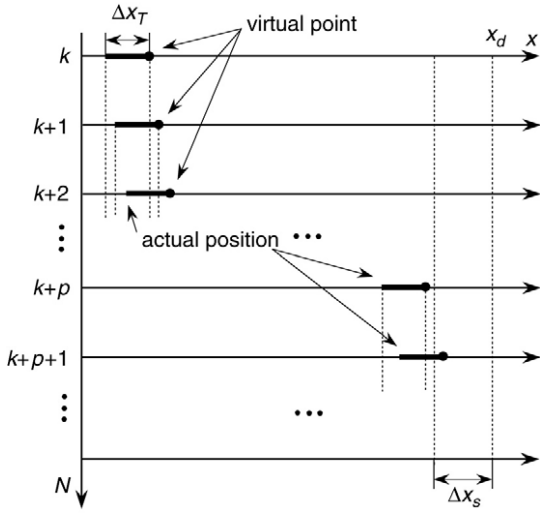

Fig. 8. A virtual point at interpolation steps $k, k+1, \ldots$.

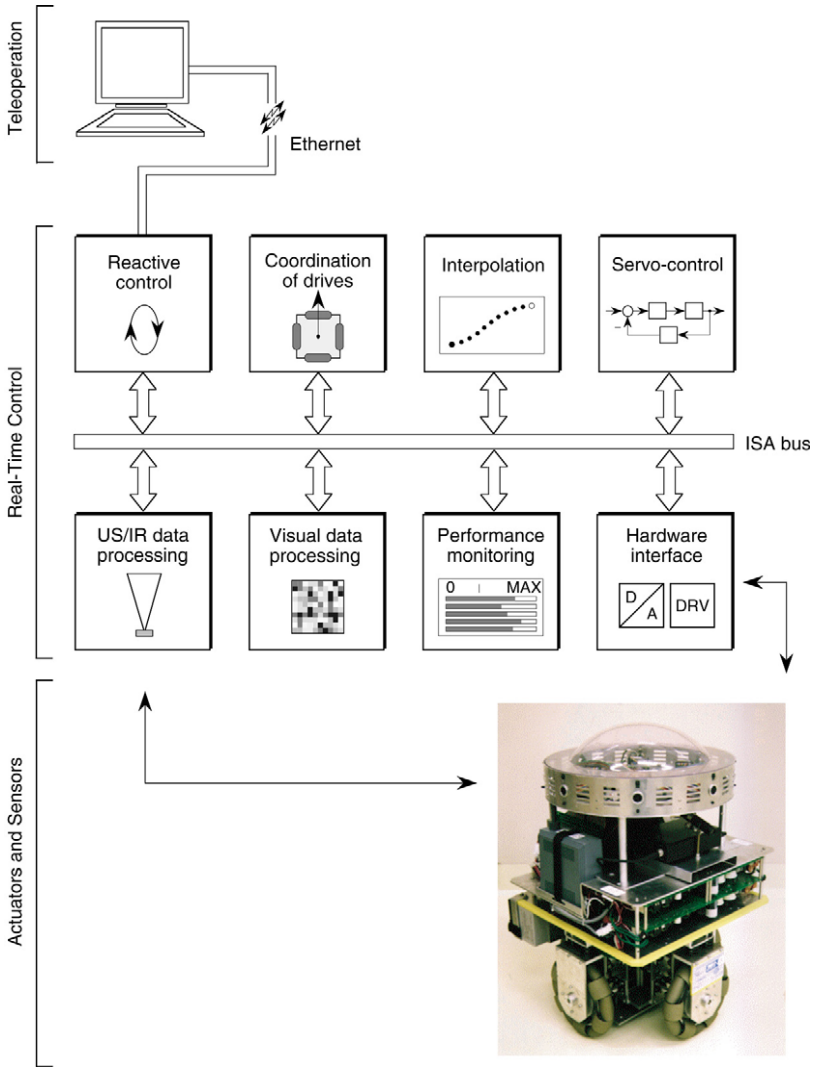

Fig. 9. The overall architecture of our mobile robot.

has its extremal value at the moment when a new $\dot{x}_d$ is set, i.e. in the beginning of the interpolation step. According to (22), for given $\dot{x}_d$ and $\dot{x}(kT^\star)$, there can always be found such $\Delta x_T \neq 0$ that the condition (17) is satisfied. One should note that, because $\tau \ll 1$, Eq. (22) can be approximated:

$$\ddot{x}(kT^\star) \approx \frac{8\dot{x}_d}{3\,\Delta x_T}\left(\dot{x}_d - \dot{x}(kT^\star)\right). \tag{23}$$

The features of this motion generation are summarized as follows: $x(t)$ and $\dot{x}(t)$ are continuous; $\dot{x}(t)$ tends to a given value and has a trapezoidal profile while the convergence speed depends on Δx_T; and $\ddot{x}(t)$ is limited and tends to zero while $\dot{x}(t)$ tends to a given value.

6. Experiments

The overall architecture of our experimental mobile robot is shown in Fig. 9 and involves: the vehicle with its actuators and sensors; the on-board control system; and the remote control interface. The reactive control ensures autonomous operation of the robot in a dynamic environment. The collision avoidance algorithm operates with a rule matrix obtained from an adaptive behavior acquisition scheme which is based on reinforcement learning. The reactive control processes data gathered by the ultrasonic and infrared sensors as well as the color CCD camera. Based on the sensors' configuration, eight possible directions of motion are considered [22]. The reactive control algorithm ensures collision-free motion to a given target position.

The robot controller provides coordinated translation and rotation of the omni-directional vehicle when moving to a target position. The controller also ensures attaining the desired velocity by the robot, as explained in Section 5.2. Omni-directional motion (holonomic case) or constrained motion (non-holonomic case) can be performed according to the assigned task. For instance, vision-based tracking of a dynamic object requires the object to be kept in the field of view of the on-board CCD camera and is achieved by the coordinated control of the translational and rotational coordinates of the robot.

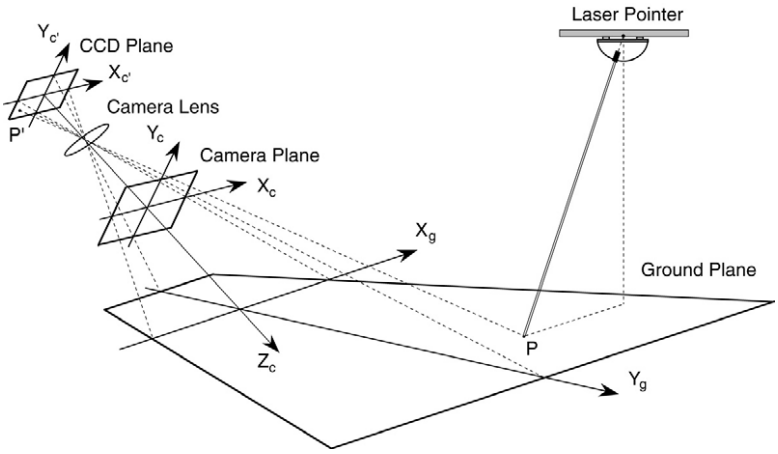

Fig. 10. A sketch of the experimental setup.

The performance monitoring aims to increase the reliability and safety of the robot's operation. The monitoring of measurable signals allows fault detection and diagnosis in a closed loop during operation, e.g. measuring the capacity level of the electric batteries of the robot and, if needed, requesting the control system to interrupt execution of the on-going task and direct the robot to a location where the electric batteries can be replaced.

The robot is equipped with a CCD color camera (focal length 7.5 mm) which is in the inclined position relative to the ground. A laser pointer (wavelength 635 nm, power output 2 mW, class I) is mounted on top of a Canon VC-C1 communication camera, as shown in Fig. 2. The laser pointer provides a red light with a spot 1 mm in diameter at a distance of 1 m. The Canon communication camera is equipped with a pan-tilt mechanism with two stepping motors. The robot's software is developed in C language and runs under the VxWorks operating system. The software of the guidance and teleoperation system is written in JAVA language and runs under the Linux operating system.

6.1. Localization of a laser beacon

The detection of the laser beacon involves: edge detection (differencing and search for pixels where the maximal change of intensity of a red color occurs); image segmentation (global thresholding to evaluate the neighboring pixels relative to a given color threshold and estimate the size of the detected areas); and selection of pixels according to a given range of the chromaticity values [23].

Our experimental setup is sketched in Fig. 10, where P denotes a position of the laser beacon seen in the image as a bright spot of the size of a few pixels, as illustrated in Fig. 11. The laser spot has a blurred contour and the shape of the beacon is elliptical, as shown in Fig. 12, where the grid represents pixels. The central part of the beacon in the image is white-colored, which shows saturation of the camera. The pixels indicated by bold contours in Fig. 12 illustrate the horizontal and vertical differencing applied in order to find the pixels where the intensity change of a red color is maximal.

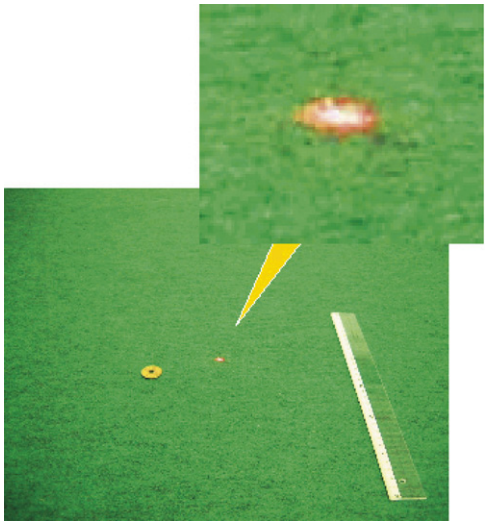

Fig. 11. A camera snapshot of the ground: a laser beacon (in the center and zoomed above), a 5 Yen coin (left) and a 30 cm ruler (right).

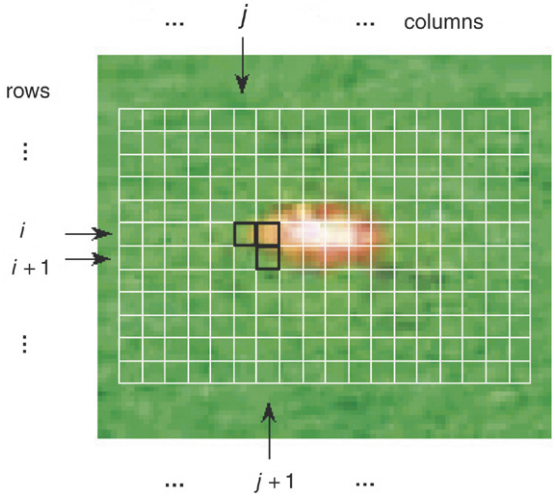

Fig. 12. A laser beacon (zoomed part of the image).

Edge detection aims to obtain the pixel coordinates of the horizontal and vertical edges of the laser beacon. Each pixel

represents the intensity of red, green and blue colors. The distribution of a red color in the image is given by a matrix $R = \{r_{ij}\}$, where $0 \leq r_{ij} \leq 255$ is the intensity of red color at a pixel (i, j). Edge detection is performed by means of the differencing of adjacent pixels of columns and rows of a matrix R: $R_h = \{r_{ij} - r_{i,j+1}\}$ and $R_v = \{r_{ij} - r_{i+1,j}\}$. The maximal value r_{nm} of matrices R_h and R_v gives the coordinates (n, m) of the pixel where the intensity change of a red color is maximal.

If the obtained intensity r_{nm} exceeds a threshold $r^\star$, the neighboring pixels of a pixel (n, m) are evaluated. An area $R_s \subset R$ is selected around a pixel (n, m) such that $\forall i, j$, $|r_{nj} - r_{nm}| < \Delta r^\star$ and $|r_{im} - r_{nm}| < \Delta r^\star$, where $\Delta r^\star$ is a given threshold. The coordinates (i, j) of the selected pixels are: $n_{\min} \leq i \leq n_{\max}$ and $m_{\min} \leq j \leq m_{\max}$. The coordinates of the central pixel (n_c, m_c) of the selected area are: $n_c = n + (n_{\max} - n_{\min})/2$ and $m_c = m + (m_{\max} - m_{\min})/2$. The size in pixels of the selected area R_s must correspond to the known average size of the laser beacon in the image. The RGB values of the pixel (n_c, m_c) are transformed into CIE chromaticity values in order to check if they correspond to the chromaticity values of the laser. Finally, coordinates (n_b, m_b) of the central pixel in the saturated area are obtained from the edge pixels. The chromaticity values of the central pixel are computed as an average of the corresponding chromaticity values of the edge pixels.

Note that differencing is performed on one image at a time, rather than differencing two sequential images (one captured when the laser light is turned on and another auxiliary image when the light is turned off). Albeit processing two images would simplify detection of the laser beacon, this introduces a delay related to communication with the guidance system and processing the auxiliary image. Since our objective is to detect the laser beacon without stopping robot motion, the above procedure is used.

In order to transform the coordinates (n_b, m_b) from pixels into meters, the camera model makes use of a plane-to-plane homography [24]. The accuracy of localizing the laser beacons on the ground relative to the robot's camera is illustrated in Fig. 13, where the ground coordinates of the camera are in the origin of the coordinate system and the camera is inclined, as shown in Fig. 10. The positions where the laser light is projected are shown as points, and the plus signs show the coordinates estimated by image processing. The accuracy is lower at the borders of the camera's field of view because of distortion (upper and lower points along the abscissae axis in Fig. 13). While the accuracy along the optical axis of the camera (central points along the abscissae axis) is sufficient for tracking the beacons: maximal dispersion was less than 10 mm and average dispersion was about 3 mm. For a smooth path specified by a sequence of beacons, as depicted in Fig. 5, tracking precision is affected by the accuracy of localizing the beacon along the optical axis of the camera: when the robot approaches the path, the image of the subsequent beacon appears closer to the central area corresponding to the optical axis of the camera. A rectification procedure will reduce image distortion if higher accuracy is required. Note that the detection

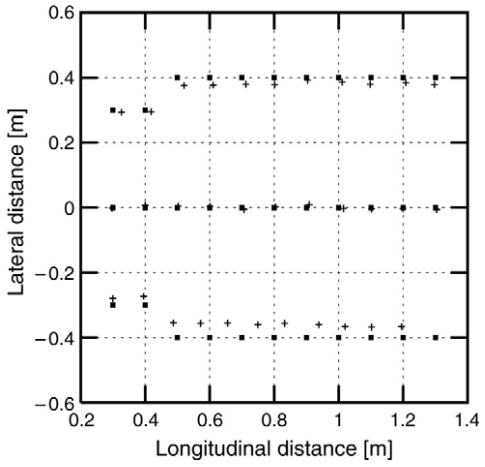

Fig. 13. Localization of projected laser beacons (the camera is at the origin in an inclined position and looks along the abscissae axis).

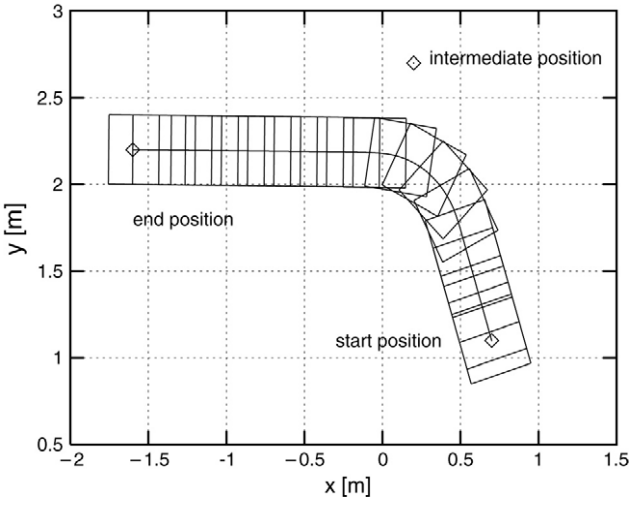

Fig. 14. Example of robot motion on the (x, y)-plane.

of a laser beacon depends on the lighting conditions, the surface material, the laser power output, and the camera sensitivity. The localization accuracy is influenced by quantization errors due to the small size of the beacon, camera displacement from the calibrated setting, and camera constraints [25].

6.2. Motion generation

The motion generation by the robot's control system is illustrated in Figs. 14 and 15. The desired maximum translational and rotational velocities are set at 0.15 m/s and 0.28 rad/s, respectively. While the robot is moving from a start position toward an intermediate position, a new target position is set ("end position" in Fig. 14). The robot abandons its intermediate position, changes its orientation and moves toward the end position. The corresponding velocity profiles (v_x, v_y, v_θ) are near trapezoidal, as shown in Fig. 15, and the desired velocities are maintained. This experiment shows that the motion generation developed is suitable for controlling the robot in a dynamic environment, in particular for tracking a moving object such as a laser beacon.

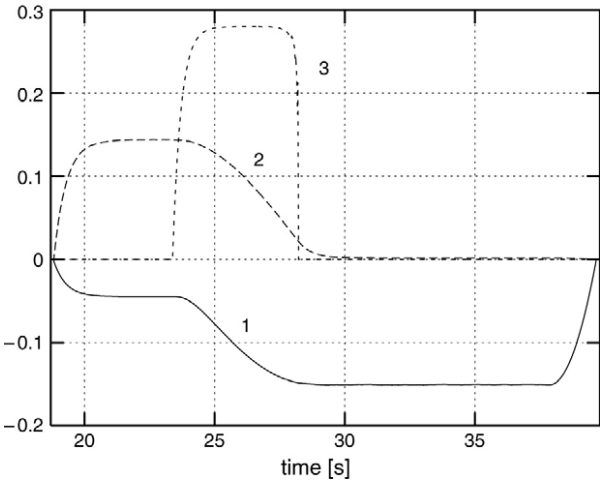

Fig. 15. Velocity profiles: 1, $v_x(t)$ in m/s; 2, $v_y(t)$ in m/s; and 3, $v_\theta(t)$ in rad/s.

6.3. Discrepancy estimation

Obtain the discrepancy between the target coordinates received from the guidance system numerically and those computed during the optical guidance by means of image processing. Since the laser system can be set precisely in the environment and localizing the laser beacon is accurate, the obtained discrepancy reflects the accumulated positional and orientational errors caused by wheels sliding on the ground, inaccurate modeling, and the system dynamics. Note that modeling of these errors would bring uncertainty into the guidance.

Initially, the coordinate systems of the robot and that of the guidance system ("world" coordinates) coincide. In order to obtain the discrepancy, each target position is informed to the robot in two ways concurrently: (1) numerically, i.e. (x, y)-coordinates are transmitted to the robot via wireless communication, and (2) optically, i.e. the same target position is shown by means of a laser beacon. The robot follows the laser beacons according to the proposed method. The coordinates computed from image processing and those received explicitly from the guidance system are memorized in order to obtain the discrepancy.

A motion segment after the robot has traveled some distance from the calibrated pose is depicted in Fig. 16. This figure shows what would happen if the robot would be guided by numerical coordinates only. The accumulated discrepancy is represented by the vertical dashed lines and it varies during the motion. The comparison of the optical and numerical guidance in Fig. 16 shows the advantage of the proposed method. The accumulated discrepancy does not affect the accuracy of guidance if the target position is shown to the robot by means of the laser beacon instead of commanding it numerically. Note that the estimation of discrepancy is not needed for optical guidance.

7. Conclusion

A novel optical guidance method for robots capable of vision and communication was proposed to improve the accuracy of guidance. The key idea of this method is to indicate interactively the feasible reference path by means of laser beacons. Optical guidance was considered as an event-driven process based on image processing and communication. The modified spline interpolation provided the feasible reference path and smooth motion trajectories. The method was illustrated in practice using a laser to guide an omni-directional mobile robot in an environment that was unknown to the robot. The architecture and models of the laser guidance system and the robot were described. Image processing for detecting and localizing the laser beacon was discussed. The experimental results have shown the effectiveness of this guidance method in improving the accuracy of robot motion.

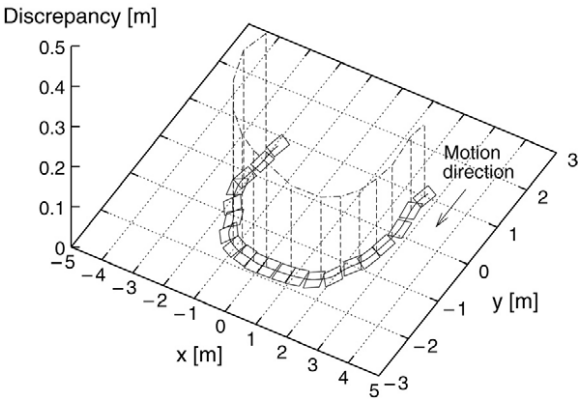

Fig. 16. A motion segment after the robot has traveled some distance from the calibrated pose under optical guidance (solid curve), and the discrepancy that would have accumulated if the numerical commands were used (vertical dash lines).

Acknowledgements

Thanks are given to Hajime Asama (the University of Tokyo), Tsuyoshi Suzuki (Tokyo Denki University) and Hayato Kaetsu (RIKEN) for their encouragement during this work.

References

[1] A. Hornby, Oxford Advanced Learner's Dictionary of Current English, Oxford University Press, 1987.
[2] I.E. Paromtchik, H. Asama, Method and System of Optical Guidance of Mobile Body, US Patent 6,629,028, 2003.
[3] I.E. Paromtchik, H. Asama, I. Endo, Moving Route Control Method by Spline Interpolation, Japan Patent 3394472, 2003.
[4] I.E. Paromtchik, H. Asama, Optical guidance system for multiple mobile robots, in: Proc. of the IEEE Int. Conf. on Robotics and Automation, Seoul, Korea, 2001, pp. 2935–2940.
[5] Y.U. Cao, A.S. Fukunaga, A.B. Kahng, Cooperative mobile robotics: Antecedents and directions, Autonomous Robots (4) (1997) 7–27.
[6] J. Borenstein, H. Everett, L. Feng, Navigating Mobile Robots—Systems and Techniques, A K Peters, Wellesley, MA, USA, 1996.
[7] M. Hebert, Active and passive range sensing for robotics, in: Proc. of the IEEE Int. Conf. on Robotics and Automation, San Francisco, CA, USA, 2000, pp. 102–110.
[8] R. Smith, M. Self, P. Cheeseman, Estimating uncertain spatial relationships in robotics, in: I. Cox, G. Wilfong (Eds.), Autonomous Robot Vehicles, Springer Verlag, 1990, pp. 167–193.
[9] J. Castellanos, J. Tardós, Mobile Robot Localization and Map Building: A Multisensor Fusion Approach, Kluwer Academic Publishers, Boston, 2000.

[10] S. Thrun, A probabilistic on-line mapping algorithm for teams of mobile robots, International Journal of Robotics Research 20 (5) (2001) 335–363.
[11] H. Choset, K. Nagatani, Topological simultaneous localization and mapping (SLAM): Toward exact localization without explicit localization, IEEE Transactions on Robotics and Automation 17 (2) (2001) 125–137.
[12] S. Hutchinson, G. Hager, P. Corke, A tutorial on visual servo control, IEEE Transactions on Robotics and Automation 12 (5) (1996) 651–670.
[13] P. Corke, Visual Control of Robots: High-Performance Visual Servoing, Research Studies Press Ltd., 1997.
[14] A. Nakamura, T. Arai, T. Hiroki, J. Ota, Development of a multiple mobile robot system controlled by a human—realisation of object command level, in: Distributed Autonomous Robotic Systems 4, 2000, pp. 208–218.
[15] J.-H. Lee, N. Ando, T. Yakushi, K. Nakajima, T. Kagoshima, H. Hashimoto, Applying intelligent space to warehouse—the first step of intelligent space project, in: Proc. of the IEEE/ASME Int. Conf. on Advanced Intelligent Mechatronics, Como, Italy, 2001, pp. 290–295.
[16] J. Redd, C. Borst, R. Volz, L. Everett, Remote Inspection System for Hazardous Sites, National Resource Center for Plutonium, Amarillo, TX, USA, 1999.
[17] M. Seelinger, E. González-Galván, M. Robinson, S. Skaar, Towards a robotic plasma spraying operation using vision, IEEE Robotics and Automation Magazine (12) (1998) 33–49.
[18] J. Ackermann, J. Guldner, W. Sienel, R. Steinhauser, V. Utkin, Linear and nonlinear controller design for robust automatic steering, IEEE Transactions on Control Systems Technology 3 (4) (1995) 132–142.
[19] H. Asama, M. Sato, L. Bogoni, H. Kaetsu, A. Matsumoto, I. Endo, Development of an omni-directional mobile robot with 3 DOF decoupling drive mechanism, in: Proc. of the IEEE Int. Conf. on Robotics and Automation, Nagoya, Japan, 1995, pp. 1925–1930.
[20] I.E. Paromtchik, H. Asama, A motion generation approach for an omnidirectional mobile robot, in: Proc. of the IEEE Int. Conf. on Robotics and Automation, San Francisco, CA, USA, 2000, pp. 1213–1218.
[21] I. Bronshtein, K. Semendyayev, Handbook of Mathematics, Verlag Harri Deutsch, Van Nostrand Reinhold Co., Edition Leipzig, 1985.
[22] Y. Arai, T. Fujii, H. Asama, Y. Kataoka, H. Kaetsu, A. Matsumoto, I. Endo, Adaptive behaviour acquisition of collision avoidance among multiple autonomous mobile robots, in: Proc. of the IEEE/RSJ Int. Conf. on Intelligent Robots and Systems, Grenoble, France, 1997, pp. 1762–1767.
[23] D. Marr, Vision, W.H. Freeman and Co., New York, 1982.
[24] J. Semple, G. Kneebone, Algebraic Projective Geometry, Oxford University Press, 1979.
[25] C. Yang, F. Ciarallo, Optimized sensor placement for active visual perception, Journal of Robotic Systems 18 (2001) 1–15.

Igor E. Paromtchik received an M.S. degree in Radio-Physics and a Ph.D. degree in System Analysis and Automatic Control from the Belarusian State University in 1985 and 1990, respectively. He received an M.B.A. degree from the University of Chicago in the USA in 2006. Throughout his career, Igor Paromtchik's research interests have focused on motion planning and control of robots. He taught control engineering and robotics as an Assistant Professor at the Belarusian State University from 1989 to 1992. While a Visiting Researcher at the University of Karlsruhe in Germany from 1992 to 1994, he helped to develop the control system of KAMRO, the Karlsruhe Autonomous Mobile Robot. In 1995, he became a Post-Doctoral Researcher and an Expert Engineer at INRIA Rhône-Alpes in France, where he worked on intelligent vehicles and developed driver assistance prototypes of automatic parking systems until 2002. In 1997, he began a scientific collaboration on mobile robots with RIKEN in Japan, where he is now a Research Scientist with RIKEN Brain Science Institute. His current research interests include control systems of mobile and humanoid robots, biped walking, dynamic cognition, and neural networks. Dr. Paromtchik is a member of the IEEE Robotics and Automation Society and has been involved in the program committees of several international conferences, including IEEE/RSJ IROS and DARS. He is also a member of IASTED's robotics technical committee. He has authored more than 70 research and technical publications and holds seven patents.